Inorganic Chemistry

Article

pubs.acs.org/IC

Late-Metal Nitrosyl Cations: Synthesis and Reactivity of $[Ni(NO)(MeNO_2)_3][PF_6]$

Ashley M. Wright, Guang Wu, and Trevor W. Hayton*

Department of Chemistry and Biochemistry, University of California, Santa Barbara, Santa Barbara, California 93106, United States

Supporting Information

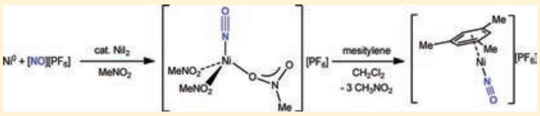

ABSTRACT: The reaction of $[NO][PF_6]$ with excess Ni powder in CH_3NO_2, in the presence of 2 mol % NiI_2, results in the formation of $[Ni(NO)(CH_3NO_2)_3][PF_6]$ (**1**), which can be isolated in modest yield as a blue crystalline solid. Also formed in the reaction is $[Ni(CH_3NO_2)_6][PF_6]_2$ (**2**), which can be isolated in comparable yield as a pale-green solid. In the solid state, **1** exhibits tetrahedral geometry about the Ni center with a linear nitrosyl ligand [Ni1−N1−O1 = 174.1(8)°] and a short Ni−N bond distance [1.626(6) Å]. As anticipated, the weakly coordinating nitromethane ligands in **1** are easily displaced by a variety of donors, including Et_2O, MeCN, and piperidine (NC_5H_{11}). More surprisingly, the addition of mesitylene to **1** results in the formation of an η^6-coordinated nickel arene complex, $[Ni(\eta^6\text{-}1,3,5\text{-}Me_3C_6H_3)(NO)][PF_6]$ (**6**). In the solid state, complex **6** exhibits a long $Ni-C_{cent}$ distance [1.682(2) Å], suggesting a relatively weak Ni−arene interaction, a consequence of the strong π-back-donation to the nitrosyl ligand. The addition of anisole to **1** also results in the formation of a η^6 nickel arene complex, $[Ni(\eta^6\text{-}MeOC_6H_5)(NO)][PF_6]$ (**7**). This complex also exhibits a long $Ni-C_{cent}$ distance [1.684(1) Å].

■ INTRODUCTION

The reaction of an electrophilic late-metal nitrosyl with a carbon nucleophile holds considerable promise as an efficient means for C−N bond formation.[1−4] Metal nitrosyls of groups 8 and 9 have been the most extensively studied as sources of electrophilic nitrosyl ligands.[1,4,5] For example, Meyer and co-workers observed the selective nitrosation at the para position of *N*,*N*′-dimethylaniline (DMA) using the ruthenium nitrosyl $[Ru(bipy)_2Cl(NO)]^{2+}$.[6,7] Additionally, Onishi et al. showed that $TpRuCl_2(NO)$ activates a vinyl C−H bond of vinylpyridine to form the nitrosoalkene complex $TpRuCl\{\kappa^2\text{-}N(=O)CH=CH(NC_5H_3R)\}$ (R = H, Me, Et).[8] Other carbon nucleophiles will also react with group 8 nitrosyls,[1,6,9,10] including enols and allylidenearylhydrazones, to give oximes[6,10] and arylazooximes, respectively.[11] Dinitrosyls of groups 8 and 9 have also proven to be reactive starting materials. For example, strained alkenes react with $[CpCo(NO)]_2$ or $RuCl_2(NO)_2(L)$ (L = tetramethylethylenediamine or 2,2′-bipyridine) to form the corresponding dinitrosoalkane complexes.[12−14]

In contrast to the chemistry reported for groups 8 and 9, the reactivity of group 10 metal nitrosyls with nucleophiles has not been well explored, in part because of the relative rarity of these complexes.[3,15] However, there are a handful of reports that detail the reactivity of nickel nitrosyls with nucleophiles.[16−19] For instance, CpNiNO reacts with RLi (R = Ph, ^{t}Bu) to form a trinuclear bridging imido complex, $[Cp_3Ni_3(\mu_3\text{-}NR)]$, as the isolated product.[16] This reaction is thought to proceed via nucleophilic attack at the N atom of the NO ligand. Moreover, the addition of NO to $[NiBr(C_3H_5)_2]_2$ results in the formation of 3-oximinopropene.[17] While the mechanism of this transformation was not fully elucidated, it was proposed to proceed through a Ni−NO intermediate. Finally, Warren and co-workers reported that the addition of ArNO (Ar = 3,5-$Me_2C_6H_3$) to $[Ar_2nacnac]NiNO$ ($Ar_2nacnac$ = ArNC(Me)CHC(Me)NAr; Ar = 2,6-^{i}$Pr_2C_6H_3$) gives $[Ar_2nacnac]Ni(\kappa^2\text{-}ONN(Ar)O)$ as the isolated product.[18]

Recently, we synthesized a copper nitrosyl complex with a rare $\{CuNO\}^{10}$ configuration, namely, $[Cu(CH_3NO_2)_5(NO)][PF_6]_2$, by the addition of $[NO][PF_6]$ to Cu powder.[20] This complex readily reacts with mesitylene to produce the donor−acceptor complex $[1,3,5\text{-}Me_3C_6H_3,NO][PF_6]$ and a copper(I) arene π complex, $[Cu(\eta^2\text{-}1,3,5\text{-}Me_3C_6H_3)_2][PF_6]$. While this transformation is consistent with the presence of an electrophilic nitrosyl ligand in $[Cu(CH_3NO_2)_5(NO)][PF_6]_2$, we observe no evidence for C−N bond formation during the reaction. Therefore, we sought to expand our investigation of late-metal nitrosyl cations to group 10 by targeting the synthesis of a nickel nitrosyl cation. Herein, we detail the synthesis of $[Ni(NO)(CH_3NO_2)_3][PF_6]$ and explore its reactivity with a variety of Lewis bases and arenes.

■ RESULTS AND DISCUSSION

Following the methodology used to synthesize $[Cu(CH_3NO_2)_5(NO)][PF_6]_2$,[20] $[NO][PF_6]$ was treated with excess Ni powder in CH_3NO_2. Surprisingly, no reaction was observed under these conditions. However, a reaction could be induced by the addition of 2 mol % of NiI_2 to the mixture. Immediately upon the addition of NiI_2, gas evolution is observed concomitant with the formation of a red solution. This solution transforms to a bright-green color within a few minutes, and after 10 min, the solution becomes blue. Workup of the reaction mixture after 1 h of stirring results in the isolation of blue crystals of $[Ni(NO)(CH_3NO_2)_3][PF_6]$ (**1**) in

Received: August 21, 2011
Published: October 27, 2011

dx.doi.org/10.1021/ic201821t | *Inorg. Chem.* 2011, 50, 11746−11753

18% yield (eq 1). Interestingly, the addition of 2 mol % I_2 to the reaction mixture also results in the formation of complex **1**,

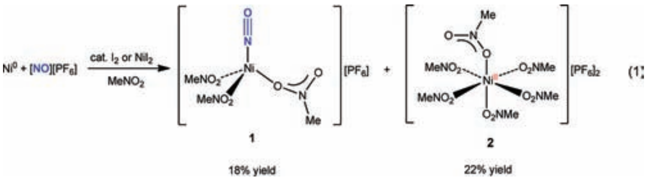

with isolated yields comparable to the NiI_2-mediated transformation. In contrast, the addition of 4 mol % $NiCl_2$ does not lead to any observable reaction after 1 h.

Complex **1** is extremely air- and moisture-sensitive in both solution and the solid state. It is also temperature-sensitive, decomposing to an intractable oil after 24 h at ambient temperature. However, it is indefinitely stable at −25 °C in the solid state. In contrast to the related copper analogue,[20] complex **1** is stable under a dynamic vacuum. In solution, **1** exhibits a high ν_{NO} absorption feature in its IR spectrum (1877 cm^{-1}, CH_2Cl_2). This ν_{NO} value is higher than those observed for previously reported nickel nitrosyls (1568−1867 cm^{-1})[18,21−40] and can be attributed to the weak Lewis basicity of CH_3NO_2 and its overall cationic charge.[41] In contrast, this value is lower than that of $[Cu(CH_3NO_2)_5(NO)][PF_6]_2$ (1933 cm^{-1}, CH_3NO_2).[20] The ^1H NMR spectrum of complex **1** in CD_2Cl_2 exhibits a singlet at 4.57 ppm, assignable to coordinated CH_3NO_2. Additionally, a broad doublet in its ^{19}F NMR spectrum at −76.7 ppm reveals the presence of PF_6^-.

Blue needles of **1** suitable for X-ray diffraction analysis were grown from CH_2Cl_2/hexane at −25 °C. Complex **1** crystallizes in the hexagonal space group $P6_5$ as a hexane solvate, $\mathbf{1}\cdot 0.16C_6H_{14}$. Its solid state molecular structure reveals a discrete cation−anion pair (Figure 1). The cationic Ni center is coordinated by one nitrosyl ligand and three CH_3NO_2 ligands, in a highly distorted tetrahedral geometry. This is evidenced by large N−Ni−L angles (av. 127.9°), a feature common to many $[Ni(NO)L_3]^+$ and $Ni(NO)L_2X$ complexes.[2,3] The metrical parameters of the Ni−N−O moiety [Ni1−N1 = 1.626(6) Å; N1−O1 = 1.139(9) Å; Ni1−N1−O1 = 174.1(8)°; Table 1] are within the range observed for other four-coordinate cationic $\{NiNO\}^{10}$ complexes.[22,23,32−34,42−44] Notably, the metrical parameters of the linear NO moiety in **1** are much different from those observed for the copper analogue $[Cu(CH_3NO_2)_5(NO)][PF_6]_2$, which contains a much longer M−N bond and a bent nitrosyl ligand.[20] Under the electron-counting rules normally used for linear nitrosyl ligands,[2] complex **1** should be described with a $Ni^0-(NO^+)$ electronic structure. This leads to the curious observation that the reaction of Ni powder with $[NO][PF_6]$ does not result in the formal oxidation of the metal. That said, assigning oxidation states in nitrosyl complexes is a challenging endeavor, an observation that resulted in the development of the Enemark−Feltham notation.[45] Accordingly, the Ni^0 oxidation state assignment for **1** is likely an oversimplification.[28] Finally, the Ni−O bond lengths in **1** range from 2.031(5) to 2.053(4) Å and are comparable to the Cu−O bond distances in $[Cu(CH_3NO_2)_5(NO)][PF_6]_2$.[20] Structurally characterized nitromethane complexes are uncommon. Previously reported examples are limited to $[TiCl_3(CH_3NO_2)]_2(\mu\text{-}Cl)_2$,[46] $AlCl_3(CH_3NO_2)$,[47] $Cu(NO_3)_2\cdot CH_3NO_2$,[48] $K(\eta^2\text{-}CH_3NO_2)(H_2O)_4Br\cdot H_2O$,[49] $[Cu(CH_3NO_2)_5(NO)][PF_6]_2$, and $[Cu(CH_3NO_2)_5][PF_6]_2$.[20]

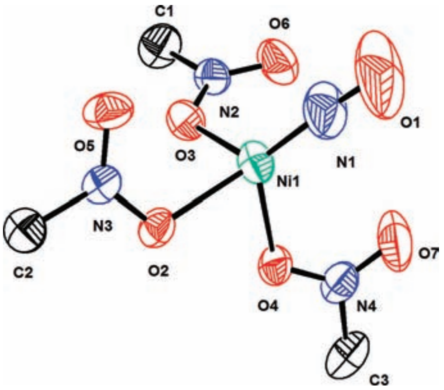

Figure 1. ORTEP drawing of $\mathbf{1}\cdot 0.16C_6H_{14}$ shown with 50% probability ellipsoids. Hexane solvate, H atoms, and $[PF_6]^-$ anion have been excluded for clarity.

In addition to complex **1**, a second product is also formed during the reaction of Ni powder with $[NO][PF_6]$, in the presence of NiI_2. This material is insoluble in CH_2Cl_2 but soluble in CH_3NO_2, permitting its separation from complex **1**. Recrystallization from CH_3NO_2/CH_2Cl_2 affords the homoleptic nitromethane complex $[Ni(CH_3NO_2)_6][PF_6]_2$ (**2**), isolated as a light-green crystalline material in 22% yield. Interestingly, if a dynamic vacuum is applied to the reaction mixture immediately after the addition of $[NO][PF_6]$ to Ni powder, complex **2** is isolated in higher yields (39%) than if the reaction is performed in a closed system. Complex **1** is not observed under these conditions. The connectivity of complex **2** has been definitively established by X-ray diffraction. However, a complete structure refinement was hampered by poor data quality. The formulation of complex **2** was also confirmed by near-IR−UV−vis spectroscopy. Three transitions at 398 nm (ε = 14 $L\cdot mol^{-1}\cdot cm^{-1}$), 664 nm ($\varepsilon$ = 6 $L\cdot mol^{-1}\cdot cm^{-1}$), and 1200 nm ($\varepsilon$ = 4 $L\cdot mol^{-1}\cdot cm^{-1}$) are consistent with those previously reported for $[Ni(CH_3NO_2)_6][SbCl_6]_2$[50,51] and closely match those of the homoleptic aquo complex $[Ni(H_2O)_6]^{2+}$.[52]

The synthesis of **1** may be mechanistically related to the synthesis of $[Ni(NO)I]_n$, which is formed by the reaction of NiI_2 with Ni powder, in the presence of NO gas.[53,54] This hypothesis is supported by the reaction of **2** with NO and Ni powder, in the presence of NiI_2 (1 mol %), which results in the formation of complex **1** in 10% yield (Scheme 1). While the yield of **1** is low under these conditions, the 1 mol % NiI_2 loading indicates that NiI_2 is acting in a catalytic fashion. Notably, the reaction does not proceed without the addition of NiI_2. Further evidence of the proposed mechanism comes from the observation that complex **1** is not formed when the reaction of Ni powder with $[NO][PF_6]$ is performed under a vacuum. Presumably, under these conditions, all of the NO gas is removed as it is formed, prohibiting the nitrosylation reaction. Also consistent with the proposed mechanism, analysis of the reaction headspace by gas-phase IR spectroscopy reveals the presence of NO gas. Surprisingly, however, N_2O is also observed, which may arise via an Ni-mediated NO coupling reaction.[54] The role of NiI_2 in the transformation is not entirely clear, but because it is required for both oxidation of the Ni powder and nitrosylation of complex **2**, we postulate that it is necessary for the generation of a soluble Ni^I intermediate that can be either nitrosylated with NO or oxidized with NO^+. The

Table 1. Selected Metrical Parameters for Complexes $1\cdot0.16C_6H_{14}$, 3, and $4\cdot0.33CH_2Cl_2$

bond lengths (Å) and angles (deg)	$1\cdot0.16C_6H_{14}$	3	$4\cdot0.33CH_2Cl_2$
Ni1−N1	1.626(6)	1.619(4)	1.633(3)
N1−O1	1.139(9)	1.160(5)	1.158(4)
Ni1−N1−O1	174.1(8)	169.6(4)	176.0(3)
Ni−L	Ni1−O2 = 2.053(4)	Ni1−O2 = 2.042(3)	Ni1−N2 = 1.981(3)
	Ni1−O3 = 2.031(5)	Ni1−O3 = 2.067(3)	Ni1−N3 = 1.976(4)
	Ni1−O4 = 2.050(4)	Ni1−O4[a] = 2.018(3)	Ni1−N4 = 1.987(3)
	av. 2.045(5)		av. 1.981(4)
N1−Ni1−L	N1−Ni1−O2 = 133.2(3)	N1−Ni1−O2 = 118.8(2)	N1−Ni1−N2 = 118.5(2)
	N1−Ni1−O3 = 126.2(3)	N1−Ni1−O3 = 130.3(2)	N1−Ni1−N3 = 122.4(2)
	N1−Ni1−O4 = 124.2(3)	N1−Ni1−O4[a] = 130.4(2)	N1−Ni1−N4 = 122.9(2)

[a] Diethyl ether ligand.

Scheme 1

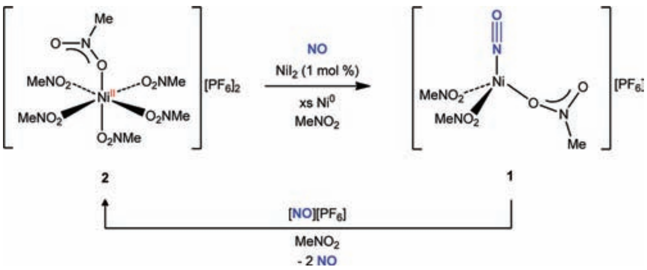

use of a weakly coordinating solvent also appears to be critical for the generation of a nitrosyl complex. When similar oxidations are performed in strongly donating solvents, such as MeCN (Gutmann donor number: MeCN = 14.1; CH_3NO_2 = 2.7),[41] they typically result in the formation of simple coordination complexes.[55] For instance, the reaction of Pd metal with 2 equiv of [NO][BF_4] in MeCN results solely in the formation of [$Pd(MeCN)_4$][BF_4]$_2$,[56] while oxidation of Ni^0 with [NO][PF_6] in MeCN leads exclusively to the formation of [$Ni(MeCN)_6$][PF_6]$_2$.[55] Also of note, oxidation of Ni powder under these conditions does not require the addition of a catalyst to proceed.[55] Finally, the reaction of complex **1** with [NO][PF_6] in $MeNO_2$ results in NO gas evolution and the formation of complex **2** in modest yield (Scheme 1). This reaction may partially explain the low yields of **1** because any [NO][PF_6] remaining in the reaction mixture would result in the reformation of **2**.

Not surprisingly, given its low donor number, the nitromethane ligands in **1** can easily be displaced with stronger Lewis bases. For example, the addition of 4 equiv of Et_2O to **1** in CH_2Cl_2 results in an immediate color change from blue to green and the appearance of a new ν_{NO} stretch at 1860 cm^{-1}. This value is 17 cm^{-1} lower than that observed for **1**. From these solutions, [$Ni(NO)(OEt_2)(CH_3NO_2)_2$][$PF_6$] (**3**) can be isolated in 50% yield (Scheme 2). In contrast, the addition of MeCN or piperidine results in the complete displacement of the CH_3NO_2 ligands, providing [$Ni(NO)(MeCN)_3$][PF_6] (**4**) and [$Ni(NO)(NC_5H_{11})_3$][PF_6] (**5**), respectively (Scheme 2). Complexes **4** and **5** exhibit ν_{NO} values of 1845 and 1772 cm^{-1} in a CH_2Cl_2 solution, respectively. Both values are substantially lower than those exhibited by complexes **1** and **3**, consistent with the stronger donating abilities of MeCN and piperidine. Moreover, the thermal stabilities of **4** and **5** are much greater than that of **1**, and they can be stored as solids at room temperature for weeks without noticeable decomposition.

Scheme 2

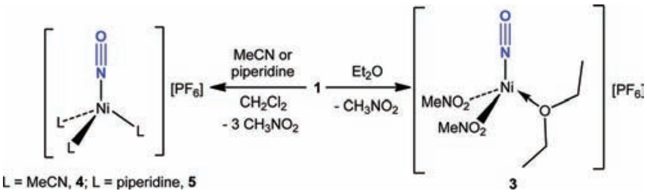

Crystals of **3** and **4** were grown by the slow diffusion of hexane into concentrated CH_2Cl_2 solutions. Complex **3** crystallizes in the monoclinic space group $P2_1/c$, while complex **4** crystallizes as a CH_2Cl_2 solvate, $4\cdot0.33CH_2Cl_2$, in the orthorhombic space group *Pnma*. Their solid-state molecular structures are shown in Figure 2, while a selection of metrical parameters are collated in Table 1. The Ni1−N1 [1.619(4) Å] and N1−O1 [1.160(5) Å] bond lengths in **3** are identical with those found in **1**, while the Ni−N−O bond angle [169.6(4)°] deviates slightly from that seen in the parent complex. The substitution of a CH_3NO_2 ligand with Et_2O lowers the symmetry of the complex from C_{3v} to C_s, which results in the splitting of degenerate dπ orbitals and accounts for deviations in the Ni−N−O angle away from 180°.[57] In the solid state, complex **4** contains two independent molecules in the asymmetric unit, one of which lies on a special position. Both exhibit similar metrical parameters, and only one will be discussed in detail. The monocationic Ni center in **4** is coordinated by one NO ligand and three MeCN ligands in a distorted tetrahedron (av. $N-Ni-N_{MeCN}$ = 121.3°). The $Ni-N_{NO}$ [1.633(3) Å] and N−O [1.158(4) Å] bond lengths in **4**

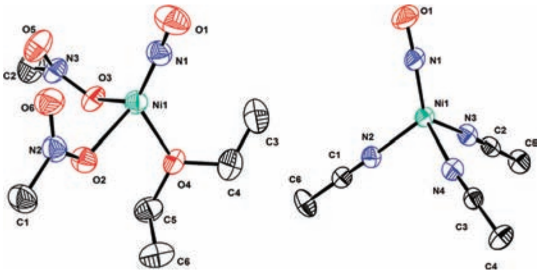

Figure 2. ORTEP drawings of **3** (left) and one of two crystallographically independent molecules of $4\cdot0.33CH_2Cl_2$ (right) shown with 50% probability ellipsoids. Hydrogen atoms and $[PF_6]^-$ anions have been excluded for clarity.

are comparable to those observed in **1** and **3**, while the Ni−N_{MeCN} bond lengths range from 1.976(4) to 1.987(3) Å.

The high ν_{NO} value observed for complex **1** suggests that its nitrosyl ligand may be susceptible to reactions with nucleophiles.[1,4,5,58,59] With this in mind, we investigated its reactivity with a variety of activated arenes.[7] Thus, the addition of 7 equiv of mesitylene to **1** in CH_2Cl_2 results in a dramatic color change from blue to red. The in situ IR spectrum of this solution features a new NO absorption feature at 1910 cm^{-1}, assignable to $[Ni(\eta^6\text{-}1,3,5\text{-}Me_3C_6H_3)(NO)][PF_6]$ (**6**). Notably, this is a higher ν_{NO} stretch than that observed for complex **1**. No evidence for NO activation, including the formation of the electron donor−acceptor complex $[1,3,5\text{-}Me_3C_6H_3,NO][PF_6]$, is observed in these solutions.[20] Complex **6** can be isolated in 71% yield by crystallization from CH_2Cl_2/hexane (eq 2). Its ^1H NMR spectrum (CD_2Cl_2) exhibits two singlets at 2.76 and 7.11 ppm, in a 3:1 ratio, respectively, assignable to the methyl and aryl protons of coordinated mesitylene.

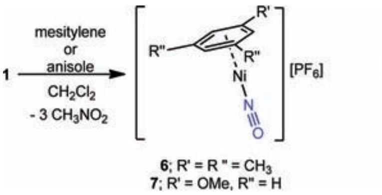

(2)

Other arenes are also capable of binding to the $[Ni(NO)]^+$ fragment in a η^6 fashion. For example, the addition of 3 equiv of anisole to **1** in CH_2Cl_2 results in the formation of $[Ni(\eta^6\text{-}MeOC_6H_5)(NO)][PF_6]$ (**7**), which can be isolated in 48% yield by crystallization from CH_2Cl_2/hexane (eq 2). Similarly, the addition of 1 equiv of DMA to complex **6** in CH_2Cl_2 results in the displacement of mesitylene and the formation of $[Ni(\eta^6\text{-}C_6H_5NMe_2)(NO)][PF_6]$ (**8**), which can be isolated as a red solid in 57% yield. The solution IR spectrum of **7** exhibits a higher ν_{NO} value (1915 cm^{-1}, CH_2Cl_2) than either **1** or **6**, while the solution IR spectrum of **8** features a ν_{NO} value of 1894 cm^{-1} (CH_2Cl_2). As determined by IR spectroscopy, there is no evidence for NO activation upon the addition of either anisole or DMA to the $[Ni(NO)]^+$ fragment. Interestingly, the addition of excess DMA to **6** in CH_2Cl_2 results in the formation of a green solution. The IR spectrum of this solution features a new NO vibration at 1840 cm^{-1}, in addition to the peak attributable to **8**. Furthermore, the feature at 1840 cm^{-1} increases in intensity with increasing concentration of DMA (see the Supporting Information). We have tentatively assigned this feature to $[Ni(NO)(C_6H_5\mathit{N}Me_2)_3][PF_6]$ (**9**), the product formed by coordination of DMA to the Ni ion via the N atom. Attempts to crystallize this green material from CH_2Cl_2/hexane results in isolation of a green oil, which converts slowly to the red crystalline material of **8** upon standing, suggesting that the η^6-coordination mode is favored.

Crystals of **6** suitable for X-ray diffraction analysis were grown from a concentrated CH_2Cl_2 solution at −25 °C. Complex **6** crystallizes in the monoclinic space group $C2/c$ and exhibits a pseudotetrahedral geometry about the Ni metal center (Figure 3). The metrical parameters of the Ni−NO moiety [Ni−N = 1.610(4) Å; N−O = 1.157(4) Å; Ni−N−O = 177.4(4)°; Table 2] are comparable to those observed for **1**, **3**, and **4** and are within the expected range for a nickel nitrosyl. Most surprisingly, the $[Ni(NO)]^+$ moiety is supported by mesitylene coordinated in a η^6 fashion to the Ni center. The Ni−C bond distances are nearly equidistant, ranging from 2.172(4) to 2.212(4) Å, while the Ni−C_{cent} distance is 1.682(2) Å. Only a few examples of η^6 nickel arene complexes are known, as the η^2-coordination mode is more common.[60−64] Notably, the Ni−C_{cent} distance in **6** is significantly longer than previously reported Ni−C_{cent} distances (1.592−1.621 Å).[60−64] The elongated Ni−C distance results from the strong π-acceptor ability of NO, which reduces the Ni−arene back-bonding interaction. Further evidence for this weak interaction is revealed upon dissolution of **6** in CH_3NO_2, which results in the reformation of **1** via displacement of the mesitylene ring.

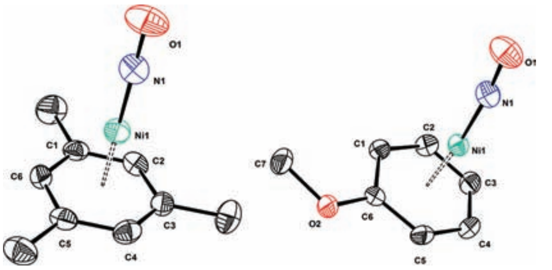

Figure 3. ORTEP diagrams of **6** (left) and **7** (right) shown with 50% probability ellipsoids. Hydrogen atoms and $[PF_6]^-$ anions have been excluded for clarity.

Table 2. Selected Metrical Parameters for Complexes 6 and 7

bond lengths (Å) and angles (deg)	6	7
C_{Ar}−C_{Ar} (av.)	1.400(7)	1.405(3)
Ni−N	1.610(4)	1.627(2)
N−O	1.157(4)	1.144(3)
Ni−N−O	177.4(4)	173.1(2)
Ni−C_{cent}	1.682(2)	1.684(1)

Complex **7** crystallizes in the monoclinic space group $P2_1/n$ (Figure 3). Its Ni−N [1.627(2) Å], N−O [1.144(3) Å], and Ni−C_{cent} [1.684(1) Å] distances are similar to those exhibited by **6**. However, the Ni−C_{aryl} bond lengths vary [from 2.152(3) to 2.253(2) Å], revealing an uncentered coordination of the ring to the Ni center. For example, the *ipso* carbon is 0.1 Å further from the Ni ion than the *para* carbon. Complexes **6** and **7** are similar to the classic "pogo-stick" complexes Cp′Ni(NO).[60,65−67] In fact, the metrical parameters of the $[Ni(NO)]^+$ moiety in **6** and **7** are comparable to those observed in Cp*Ni(NO) [Ni−N = 1.620(3) Å; N−O = 1.177(3) Å; Ni−N−O = 179.2(3)°].[67] However, the ν_{NO} values between these two classes of molecules differ by over 100 cm^{-1} [e.g., 1910 cm^{-1} for **6** vs 1787 cm^{-1} for Cp*Ni(NO)], no doubt a consequence of the positive charge on complexes **6** and **7**.

Clearly, the addition of the activated arenes to the $[Ni(NO)]^+$ fragment does not result in the desired C−N bond formation with the NO ligand. Instead, the arene ring only coordinates to the Ni ion via an η^6 interaction. Attempts to promote NO activation by heating to 60−80 °C only result in decomposition, as determined by ^1H NMR spectroscopy. Similarly, the addition of a base, such as Cs_2CO_3 or NEt_3, does not yield any tractable products. While the high ν_{NO} value for complex **1** is indicative of the presence of an electrophilic NO moiety, the Ni center is still the preferred site of reactivity in all cases, likely because of the lability of the coligands. Accordingly, future attempts to engage the NO ligand in reactivity will focus on using chelating coligands to limit access to the Ni ion.

■ SUMMARY

Reaction of Ni powder with [NO][PF_6] in CH_3NO_2, in the presence of 2 mol % NiI_2, results in nitrosylation of the metal and formation of a cationic nickel nitrosyl, [Ni(NO)(CH_3NO_2)$_3$][PF_6]. The reaction does not proceed without the addition of a catalyst, such as NiI_2, which we believe is required for the formation of a Ni^I intermediate. While the isolated yield is modest, [Ni(NO)(CH_3NO_2)$_3$][PF_6] is a good synthon for nickel nitrosyl chemistry because the weakly coordinating CH_3NO_2 ligands allow for facile displacement with a variety of donor ligands. This is manifested most dramatically by the addition of arenes to **1**, which leads to isolation of a series of η^6 nickel arene complexes, [(η^6-arene)Ni(NO)][PF_6]. These complexes are rare examples of η^6 coordination of an arene ring to a Ni center. Most importantly, the addition of these activated arenes to **1** does not result in the desired C−N bond formation with the NO ligand. This contrasts sharply with the reaction between the cationic copper nitrosyl, [Cu(CH_3NO_2)$_5$(NO)][PF_6]$_2$, and mesitylene, which results in facile NO^+ transfer from Cu to the arene ring. The differing reactivity of **1** and [Cu(CH_3NO_2)$_5$(NO)][PF_6]$_2$ possibly relates to a stronger Ni−N interaction due to better π back-donation from Ni to NO.

■ EXPERIMENTAL SECTION

General Procedures. All reactions and subsequent manipulations were performed under anaerobic and anhydrous conditions under either high vacuum or an atmosphere of nitrogen or argon. Nitromethane was recrystallized from Et_2O three times and then distilled over $MgSO_4$ or CaH_2. Hexanes and diethyl ether were dried using a Vacuum Atmospheres DRI-SOLV solvent purification system. CD_2Cl_2 and CD_3NO_2 were dried over activated 3 Å molecular sieves for 24 h before use. All other reagents were purchased from commercial suppliers and used as received. NMR spectra were recorded on a Varian UNITY INOVA 400 or a Varian UNITY INOVA 500 spectrometer. ^1H and $^{13}C\{^1H\}$ NMR spectra were referenced to external $SiMe_4$ using the residual protio solvent peaks as internal standards (^1H NMR experiments) or the characteristic resonances of the solvent nuclei (^{13}C NMR experiments). $^{19}F\{^1H\}$ NMR spectra were referenced to external CCl_3F. $^{31}P\{^1H\}$ NMR spectra were referenced to external 85% H_3PO_4. IR spectra were recorded on a Mattson Genesis FTIR or a Thermo Scientific Nicolet 6700 FTIR spectrometer, while UV−vis experiments were performed on a UV-3600 Shimadzu spectrophotometer. Elemental analyses were performed by the Microanalytical Laboratory at University of California, Berkeley (Berkeley, CA).

[Ni(NO)(CH_3NO_2)$_3$][PF_6] (1). NiI_2 (14 mg, 0.045 mmol, 2 mol %) was added to excess Ni metal powder (559 mg, 9.52 mmol) in CH_3NO_2 (2 mL) in a 20 mL scintillation vial. To this suspension was added [NO][PF_6] (331 mg, 1.89 mmol). The cap was immediately fastened, and the solution was vigorously stirred. Gas evolution was observed, and a red solution quickly formed. This solution became bright green and then dark blue over the course of 10 min. After 1 h, the solvent was removed in vacuo and the residue was extracted with CH_2Cl_2 (6 mL). The solution was filtered through a Celite column (0.5 cm × 2 cm) supported on glass wool, leaving a green solid (vide infra) and excess Ni powder on the Celite plug. The solution was then concentrated and layered with hexane (5 mL). Storage at −25 °C resulted in the precipitation of blue fibrous needles that were isolated by decanting the supernatant and drying under vacuum. Yield: 18%, 144 mg. Anal. Calcd for $C_3H_9F_6N_4NiO_7P$: C, 8.65; H, 2.18; N, 13.44. Found: C, 8.74; H, 1.97; N, 12.30. ^1H NMR (CD_2Cl_2, 22 °C, 500 MHz): δ 4.57 (3H, s, CH_3NO_2). ^{19}F NMR (CD_2Cl_2, 22 °C, 470 MHz): δ −76.7 (br d, J_{PF} = 714 Hz). ^{19}F NMR (CD_3NO_2, 22 °C, 376 Hz): δ −76.7 (d, J_{PF} = 707 Hz). ^{31}P NMR (CD_2Cl_2, 22 °C, 202 MHz): δ −141.7 (sept, J_{PF} = 715 Hz). ^{31}P NMR (CD_3NO_2, 22 °C, 162 Hz): δ −144.8 (sept, J_{PF} = 706 Hz). $^{13}C\{^1H\}$ NMR (CD_2Cl_2, 22 °C, 125 MHz): δ 61.65 (CH_3NO_2). IR (Nujol mull, cm^{-1}): 1880 (s, ν_{NO}), 1565 (s), 1404 (s), 1101 (m), 849 (s), 741 (m), 657 (s), 563 (m). IR (CH_2Cl_2, cm^{-1}): 1877 (s, ν_{NO}). IR (CH_3NO_2, cm^{-1}): 1857 (s, ν_{NO}). UV−vis (CH_2Cl_2, 25 °C, 0.75 mM): 399 nm (ε = 112 L·mol^{-1}·cm^{-1}), 662 nm (ε = 266 L·mol^{-1}·cm^{-1}).

[Ni(CH_3NO_2)$_6$][PF_6]$_2$ (2). The green insoluble material generated during the synthesis of **1** was dissolved in CH_3NO_2 (2 mL) and filtered through a Celite column (0.5 cm × 2 cm) supported on glass wool. The resulting light-green solution was layered onto CH_2Cl_2 (5 mL). Storage at −25 °C resulted in the deposition of pale-green needles. These were isolated by decanting off the supernatant, washing with CH_2Cl_2 (2 × 2 mL), and drying in vacuo. Yield: 22%, 148 mg. Anal. Calcd for $C_6H_{18}F_{12}N_6NiO_{12}P_2$: C, 10.08; H, 2.54; N, 11.76. Found: C, 10.67; H, 2.70; N, 11.36. ^1H NMR (CD_3NO_2, 22 °C, 500 MHz): δ 4.34 (3H, s, CH_3NO_2). ^{19}F NMR (CD_3NO_2, 22 °C, 470 MHz): δ −69.0 (br d). ^{31}P NMR (CD_3NO_2, 22 °C, 202 MHz): δ −142.2 (sept, J_{PF} = 699 Hz). IR (Nujol mull, cm^{-1}): 1568 (s), 1385 (m), 1277 (w), 1263 (w), 1110 (m), 1044 (w), 918 (m), 837 (s), 741 (m), 671 (s), 607 (m), 558 (m). UV−vis (CH_3NO_2, 25 °C, 25.9 mM): 398 nm (ε = 14 L·mol^{-1}·cm^{-1}), 664 nm (ε = 6 L·mol^{-1}·cm^{-1}), 730 nm (ε = 5 L·mol^{-1}·cm^{-1}), 1200 nm (ε = 4 L·mol^{-1}·cm^{-1}, Δ_{oct} = 8300 cm^{-1}).

[Ni(Et_2O)(CH_3NO_2)$_2$(NO)][PF_6] (3). A solution of Et_2O (54 mg, 0.73 mmol) in CH_2Cl_2 (1 mL) was added to a stirring solution of **1** (85 mg, 0.20 mmol) in CH_2Cl_2 (1 mL). This resulted in a color change to dark turquoise. The reaction mixture was stirred for 5 min and then filtered through a Celite column (0.5 cm × 2 cm) supported on glass wool. The supernatant was layered with hexanes (2 mL), and subsequent storage at −25 °C resulted in the deposition of turquoise-blue blocks. The crystals were dried in vacuo for <1 min. Yield: 50%, 43 mg. Note: Exposure to a dynamic vacuum results in the partial loss of diethyl ether. Anal. Calcd for $C_6H_{16}F_6N_3NiO_6P$: C, 16.76; H, 3.75; N, 9.77. Found: (run A) C, 15.80; H, 3.47; N, 8.87; (run B) C, 15.72; H, 3.56; N, 9.35. ^1H NMR (CD_2Cl_2, 22 °C, 400 MHz): δ 1.63 (6H, t, OCH_2CH_3), 3.71 (4H, q, OCH_2CH_3), 4.56 (6H, s, CH_3NO_2). ^{19}F NMR (CD_2Cl_2, 22 °C, 470 MHz): δ −76.52 (J_{PF} = 724 Hz, br d). ^{13}C NMR (CD_2Cl_2, 22 °C, 125 MHz): δ 68.94 (OCH_2CH_3), 13.04 (OCH_2CH_3). ^{31}P NMR (CD_2Cl_2, 22 °C, 202 MHz): δ −140.96 (J_{PF} = 709 Hz, br sept). IR (CH_2Cl_2, cm^{-1}): 1860 (s, ν_{NO}). IR (Nujol mull, cm^{-1}): 1857 (s, ν_{NO}), 1567 (s), 1379 (s), 1192 (w), 1157 (w), 1092 (m), 1046 (m), 837 (s), 741 (w), 671 (m), 605 (w), 561 (m). UV−vis (CH_2Cl_2, 25 °C, 2.33 mM): 400 nm (ε = 69 L·mol^{-1}·cm^{-1}), 682 nm (ε = 274 L·mol^{-1}·cm^{-1}).

[Ni(MeCN)$_3$(NO)][PF_6] (4). To a stirring solution of **1** (105 mg, 0.252 mmol) in CH_2Cl_2 (1 mL) was added MeCN (77 mg, 1.9 mmol) dissolved in CH_2Cl_2 (1 mL). This resulted in a color change to dark purple-blue. The reaction mixture was stirred for 15 min and then filtered through a Celite column (0.5 cm × 2 cm) supported on glass wool. The supernatant was layered with hexanes (3 mL), and subsequent storage at −25 °C resulted in the deposition of blue needles. The supernatant was decanted, and the crystals were washed with hexanes (1 mL) and dried in vacuo for 10 min. Yield: 64%, 58 mg. Anal. Calcd for $C_6H_9F_6N_4NiOP$: C, 20.20; H, 2.54; N, 15.70. Found: C, 20.33; H, 2.45; N, 15.36. ^1H NMR (CD_2Cl_2, 22 °C, 500 MHz): δ 2.40 (3H, s, CH_3CN). ^{19}F NMR (CD_2Cl_2, 22 °C, 470 MHz): δ −74.66 (J_{PF} = 709 Hz, d). $^{13}C\{^1H\}$ NMR (CD_2Cl_2, 22 °C, 125 MHz): δ 129.24 (MeCN) 5.08 (CH_3CN). ^{31}P NMR (CD_2Cl_2, 22 °C, 202 MHz): δ −144.04 (J_{PF} = 710 Hz, sept). IR (Nujol mull, cm^{-1}): 2322 (m, ν_{CN}), 2293 (m, ν_{CN}), 1842 (s, ν_{NO}), 1828 (sh), 1304 (w), 1036 (m), 943 (w), 838 (s), 723 (m), 558 (m). IR (CH_2Cl_2, cm^{-1}): 1845 (s, ν_{NO}). IR (CH_3NO_2, cm^{-1}): 1842 (s, ν_{NO}). IR (CH_3CN, cm^{-1}): 1841 (s, ν_{NO}). UV−vis (CH_2Cl_2, 25 °C, 6.34 mmol): 381 nm (ε = 21 L·mol^{-1}·cm^{-1}), 617 nm (ε = 99 L·mol^{-1}·cm^{-1}).

[Ni(NO)(NC_5H_{11})$_3$][PF_6] (5). To a stirring CH_2Cl_2 solution (1 mL) of **1** (114 mg, 0.274 mmol) was added piperidine (77 mg, 0.90 mmol). After stirring for 5 min, the solution was filtered through a Celite column (0.5 cm × 2 cm) supported on glass wool. The supernatant was layered with hexanes (4 mL), and subsequent storage at −25 °C resulted in the deposition of dark-blue blocks. These were washed with pentane (5 mL) and dried in vacuo. Yield: 72%, 96 mg. Anal. Calcd for

Table 3. X-ray Crystallographic Data for Complexes $1{\cdot}0.16C_6H_{14}$−7

	$1{\cdot}0.16C_6H_{14}$	3	$4{\cdot}0.33CH_2Cl_2$	6	7
empirical formula	$C_4H_{11.33}F_6N_4NiO_7P$	$C_6H_{16}F_6N_3NiO_6P$	$C_{6.33}H_{9.66}Cl_{0.66}F_6N_4NiOP$	$C_9H_{12}F_6NNiOP$	$C_7H_8F_6NNiO_2P$
cryst habit, color	needle, blue	block, dark turquoise	block, blue	rod, red-orange	needle, red-orange
cryst size (mm)	0.60 × 0.20 × 0.20	0.50 × 0.30 × 020	0.50 × 0.30 × 0.20	0.20 × 0.20 × 0.10	0.60 × 0.40 × 0.20
cryst syst	hexagonal	monoclinic	orthorhombic	monoclinic	monoclinic
space group	*P*6(5)	*P*2(1)/*c*	*Pnma*	*C*2/*c*	*P*2(1)/*n*
vol (Å^3)	2272.4(2)	1605.3(2)	4432.7(6)	2606.3(10)	1139.6(2)
a (Å)	17.4863(5)	8.4116(7)	21.2921(15)	23.003(5)	10.1766(6)
b (Å)	17.4863(5)	12.0802(9)	19.4726(14)	7.983(2)	9.5538(6)
c (Å)	8.5815(5)	15.826(2)	10.6911(8)	16.518(4)	12.4940(7)
α (deg)	90	90	90	90	90
β (deg)	90	93.449(2)	90	120.773(3)	110.257(1)
γ (deg)	120	90	90	90	90
Z	6	4	4	8	4
fw (g/mol)	431.16	429.90	387.68	353.88	341.82
density (calcd, Mg/m^3)	1.880	1.779	1.728	1.804	1.992
abs coeff (mm^{-1})	1.491	1.401	1.605	1.674	1.916
F_{000}	1248	872	2296	1424	680
total no. reflns	19 641	12 843	35 152	10 337	9297
unique reflns	3093	3220	4647	2622	2352
R_{int}	0.0585	0.0754	0.1083	0.1779	0.0715
final *R* indices [$I > 2\sigma(I)$]	R1 = 0.0541, wR2 = 0.1361	R1 = 0.0563, wR2 = 0.1565	R1 = 0.0486, wR2 = 0.1069	R1 = 0.0518, wR2 = 0.1040	R1 = 0.0336, wR2 = 0.0789
largest diff peak and hole (e·Å^{-3})	0.911 and −0.362	1.061 and −0.762	0.681 and −0.623	0.550 and −0.497	0.327 and −0.532
GOF	1.087	0.983	0.973	0.937	1.061

$C_{15}H_{33}F_6N_4NiOP$: C, 36.83; H, 6.80; N, 11.45. Found: C, 36.33; H, 6.50; N, 11.05. ^{1}H NMR (CD_2Cl_2, 22 °C, 500 MHz): δ 1.83 (br s, β/γ-C*H*, 18H), 3.47 (br s, α-C*H*, 12H). NH resonances not observed. ^{13}C NMR (CD_2Cl_2, 22 °C, 125 MHz): δ 25.90 (γ-CH_2), 29.21 (β-CH_2), 53.55 (α-CH_2). ^{19}F NMR (CD_2Cl_2, 22 °C, 470 MHz): δ −72.79 (d, J_{PF} = 712 Hz). ^{31}P NMR (CD_2Cl_2, 22 °C, 202 MHz): δ −144.22 (J_{PF} = 711 Hz, sept). IR (CH_2Cl_2, cm^{-1}): 1772 (s, ν_{NO}). IR (CH_3NO_2, cm^{-1}): 1769 (s, ν_{NO}). IR (Nujol mull, cm^{-1}): 3278 (m), 2727 (w), 1757 (s, ν_{NO}), 1452 (m), 1314 (w), 1271 (m), 1191 (m), 1174 (w), 1116 (w), 1077 (m), 1040 (w), 1024 (w), 1002 (m), 946 (m), 842 (s), 740 (m), 723 (m), 557 (m). UV−vis (0.71 mM, CH_2Cl_2, 25 °C): 358 nm (ε = 265 L·mol^{-1}·cm^{-1}), 633 nm (ε = 487 L·mol^{-1}·cm^{-1}).

[Ni(η^6-1,3,5-$Me_3C_6H_3$)(NO)][PF_6] (6). To a stirring CH_2Cl_2 (2 mL) solution of **1** (105 mg, 0.251 mmol) was added mesitylene (222 mg, 1.85 mmol). This resulted in a color change to orange-red. After stirring for 2 min, the solution was filtered through a Celite column (0.5 cm × 2 cm) supported on glass wool. The filtrate was layered with hexane (2 mL), and subsequent storage at −25 °C over 24 h resulted in the deposition of orange-red needles. The crystals were washed with hexanes (1 mL) and dried in vacuo. Yield: 71%, 63 mg. Anal. Calcd for $C_9H_{12}F_6NNiOP$: C, 30.55; H, 3.42; N, 3.96. Found: C, 30.28; H, 3.43; N, 3.89. ^{1}H NMR (CD_2Cl_2, 25 °C, 500 MHz): δ 2.76 (s, ArCH_3, 9H), 7.11 (s, Ar*H*, 3H). ^{13}C NMR (CD_2Cl_2, 25 °C, 125 MHz): δ 22.26 (ArCH_3), 112.16 (^{Ar}CH), 128.52 (^{Ar}CMe). ^{19}F NMR (CD_2Cl_2, 25 °C, 470 MHz): δ −73.69 (d, J_{PF} = 710 Hz). ^{31}P NMR (CD_2Cl_2, 22 °C, 212 MHz): δ −142.52 (sept, J_{PF} = 711 Hz). IR (Nujol mull, cm^{-1}): 3067 (w), 1921 (s, ν_{NO}), 1557 (m), 1307 (w), 1035 (w), 835 (s), 740 (w), 723 (w), 678 (w), 558 (m). IR (CH_2Cl_2, cm^{-1}): 1910 (s, ν_{NO}). UV−vis (CH_2Cl_2, 25 °C, 7.41 mM): 405 nm (ε = 121 L·mol^{-1}·cm^{-1}), 487 nm (ε = 139 L·mol^{-1}·cm^{-1}), 689 nm (ε = 12 L·mol^{-1}·cm^{-1}).

[Ni(η^6-C_6H_5OMe)(NO)][PF_6] (7). To a CH_2Cl_2 solution (2 mL) of **1** (57 mg, 0.14 mmol) was added anisole (42 mg, 0.39 mmol) as a CH_2Cl_2 solution (1 mL). This resulted in a color change to orange. After stirring for 2 min, the solution was filtered through a Celite column (0.5 cm × 2 cm) supported on glass wool. The filtrate was layered with pentane (4 mL), and subsequent storage at −25 °C over 24 h resulted in the deposition of orange crystals. These were isolated by decanting off the solution and washing with hexane (1 mL). Yield: 48%, 23 mg. Anal. Calcd for $C_7H_8F_6NNiO_2P$: C, 24.60; H, 2.36; N, 4.10. Found: C, 24.47; H, 2.47; N, 4.06. ^{1}H NMR (CD_2Cl_2, 22 °C, 500 MHz): δ 4.17 (3H, s, OCH_3), 7.10 (1H, t, *J* = 7 Hz, *p*-H), 7.17 (2H, d, *J* = 8 Hz, *o*-H), 7.46 (2H, t, *J* = 7 Hz, *m*-H). ^{19}F NMR (CD_2Cl_2, 22 °C, 470 MHz): δ −72.28 (J_{PF} = 711 Hz, d). ^{13}C NMR (CD_2Cl_2, 22 °C, 125 MHz): δ 114.23 (*m*-C), 105.14 (*p*-C), 100.66 (*o*-C), 59.85 (OCH_3). The resonance for the *ipso*-C was not observed. ^{31}P NMR (CD_2Cl_2, 22 °C, 202 MHz): δ −143.94 (J_{PF} = 710 Hz, sept). IR (Nujol mull, cm^{-1}): 1918 (vs, ν_{NO}), 1629 (w), 1560 (m), 1538 (w), 1485 (w), 1326 (w), 1311 (w), 1274 (m), 1184 (w), 1174(w), 1159 (w), 1151 (w), 1070 (w), 1022 (m), 988 (w), 933 (w), 879 (sh), 834 (s), 789 (m), 740 (w), 723 (w), 558 (m). IR (CH_2Cl_2, cm^{-1}): 1915 (vs, ν_{NO}). UV−vis (3.13 mM, CH_2Cl_2, 25 °C): 414 nm (ε = 164 L·mol^{-1}·cm^{-1}), 487 nm (ε = 155 L·mol^{-1}·cm^{-1}), 690 nm (ε = 33 L·mol^{-1}·cm^{-1}).

[Ni(η^6-$C_6H_5NMe_2$)(NO)][PF_6] (8). To a CH_2Cl_2 solution (2 mL) of **6** (30 mg, 0.085 mmol) was added DMA (10 μL, 0.079 mmol). After stirring for 2 min, the solution was filtered through a Celite column (0.5 cm × 2 cm) supported on glass wool. The filtrate was layered with hexane (2 mL), and subsequent storage at −25 °C over 12 h resulted in the deposition of orange blocks. These were isolated by decanting off the solution and washing with hexane (1 mL). Yield: 57%, 16 mg. Anal. Calcd for $C_8H_{11}F_6N_2NiOP$: C, 27.08; H, 3.12; N, 7.89. Found: C, 26.76; H, 3.30; N, 7.52. ^{1}H NMR (CD_2Cl_2, 22 °C, 500 MHz): δ 3.30 (6H, s, NCH_3), 6.64 (2H, br s, *o*-H), 6.69 (1H, br s, *p*-H), 7.21 (2H, br s, *m*-H). ^{19}F NMR (CD_2Cl_2, 22 °C, 470 MHz): δ −72.60 (J_{PF} = 711 Hz, d). ^{31}P NMR (CD_2Cl_2, 22 °C, 202 MHz): δ −143.93 (J_{PF} = 710 Hz, sept). IR (Nujol mull, cm^{-1}): 3107 (w), 1892 (s, ν_{NO}), 1581 (m), 1513 (w), 1234 (m), 1194 (m), 1073 (w), 1019 (w), 1004 (w), 992 (w), 982 (w), 911 (sh), 837 (s), 808 (sh), 723 (w), 684 (w), 557 (m). IR (CH_2Cl_2, cm^{-1}): 1894 (s, ν_{NO}). UV−vis (0.29 mM, 25 °C, CH_2Cl_2): 445 nm (ε = 847 L·mol^{-1}·cm^{-1}), 700 nm (ε = 103 L·mol^{-1}·cm^{-1}).

[Ni(NO)($C_6H_5NMe_2$)$_3$][PF_6] (9). To a CH_2Cl_2 (4 mL) solution of **6** (35 mg, 0.10 mmol) was added DMA (0.31 mL, 2.45 mmol). This resulted in the formation of a dark-green solution. The solution IR spectrum exhibited two ν_{NO} features at 1895 and 1840 cm^{-1}, assignable to complexes **8** and **9**, respectively (see Figure S67 in the Supporting Information). The solution was layered with hexane (4 mL), and subsequent storage at −25 °C over 12 h resulted in the deposition of a dark-green oil. Upon standing at −25 °C for 3 weeks, this oil converted into an orange crystalline solid, which was identified as complex **8**.

X-ray Crystallography. Data for **1**·0.16C_6H_{14}, **3**, **4**·0.33CH_2Cl_2, **6**, and **7** were collected on a Bruker 3-axis platform diffractometer equipped with a SMART-1000 CCD detector using a graphite monochromator with a Mo Kα X-ray source (α = 0.710 73 Å). The crystals were mounted on a glass fiber under Paratone-N oil, and all data were collected at 150(2) K using an Oxford nitrogen gas cryostream system. A hemisphere of data was collected using ω scans with 0.3° frame widths. Frame exposures of 12, 20, 15, 15, and 20 s were used for complexes **1**·0.16C_6H_{14}, **3**, **4**·0.33CH_2Cl_2, **6**, and **7**, respectively. Data collection and cell parameter determination were conducted using the *SMART* program.[68] Integration of the data frames and final cell parameter refinement were performed using *SAINT* software.[69] Absorption correction of the data was carried out empirically based on reflection ψ scans. Subsequent calculations were carried out using *SHELXTL*.[70] Structure determination was done using direct or Patterson methods and difference Fourier techniques. All H-atom positions were idealized and rode on the atom of attachment. Structure solution, refinement, graphics, and creation of publication materials were performed using *SHELXTL*.

Data collection for **2** was performed on Mo and Cu X-ray sources; however, the diffraction data were of poor quality in both cases. Connectivity of the atoms in complex **2** was confirmed, but anomalous Q peaks in the lattice and significant disorder in the PF_6 anions resulted in unsatisfactory R1 and wR2 values. The unit cell parameters for complex **2** are a = 7.9665(2) Å, b = 45.7424(10) Å, c = 12.0144(3) Å, α = 90.00°, β = 105.040(1)°, and γ = 90.00°.

The PF_6 anion in complex **3** possessed significant rotational disorder. It was disordered over two orientations in a 50:50 ratio. The P−F bond distances were fixed at 1.57(5) Å, while the closest neighboring F-atom distances were fixed at 1.20(5) Å. The FLAT command was also performed on P1, F1A, F1B, F2A, F2B, F4A, F4B, F6A, and F6B. In addition, the PF_6 anion in complex **6** possessed rotational disorder around one axis in a 72:28 ratio. A summary of relevant crystallographic data is presented in Table 3.

■ ASSOCIATED CONTENT

Ⓢ Supporting Information

X-ray crystallographic data in CIF format, additional experimental details, and NMR and IR spectral data. This material is available free of charge via the Internet at http://pubs.acs.org.

■ AUTHOR INFORMATION

Corresponding Author

*E-mail: hayton@chem.ucsb.edu.

■ ACKNOWLEDGMENTS

We thank the University of California, Santa Barbara, for financial support of this work.

■ REFERENCES

(1) Bottomley, F. *Reactions of Coordinated Ligands*; Plenum Press: New York, 1986; Vol. 2, pp 115−222.

(2) Legzdins, P.; Richter-Addo, G. B. *Metal Nitrosyls*; Oxford University Press: New York, 1992.

(3) Hayton, T. W.; Sharp, W. B.; Legzdins, P. *Chem. Rev.* **2002**, *102*, 935−992.

(4) Doctorovich, F.; Di Salvo, F. *Acc. Chem. Res.* **2007**, *40*, 985−993.

(5) Escola, N.; Llebaria, A.; Leitus, G.; Doctorovich, F. *Organometallics* **2006**, *25*, 3799−3801.

(6) Bowden, W. L.; Little, W. F.; Meyer, T. J. *J. Am. Chem. Soc.* **1974**, *96*, 5605−5607.

(7) Bowden, W. L.; Little, W. F.; Meyer, T. J. *J. Am. Chem. Soc.* **1976**, *98*, 444−448.

(8) Arikawa, Y.; Asayama, T.; Itatani, K.; Onishi, M. *J. Am. Chem. Soc.* **2008**, *130*, 10508−10509.

(9) Lee, J.; Chen, L.; West, A. H.; Richter-Addo, G. B. *Chem. Rev.* **2002**, *102*, 1019−1066.

(10) Bottomley, F.; White, P. S. *J. Chem. Soc., Dalton Trans.* **1988**, 2965−2969.

(11) Chakravarty, A. R.; Chakravarty, A. *J. Chem. Soc., Dalton Trans.* **1983**, 961−966.

(12) Weiner, W. P.; White, M. A.; Bergman, R. G. *J. Am. Chem. Soc.* **1981**, *103*, 3612−3614.

(13) Schomaker, J. M.; Boyd, W. C.; Stewart, I. C.; Toste, F. D.; Bergman, R. G. *J. Am. Chem. Soc.* **2008**, *130*, 3777−3779.

(14) Crimmin, M. R.; Bergman, R. G.; Toste, F. D. *Angew. Chem., Int. Ed.* **2011**, *50*, 4484−4487.

(15) Doyle, M. P.; Siegfried, B.; Hammond, J. J. *J. Am. Chem. Soc.* **1976**, *98*, 1627−1629.

(16) Müller, J.; Dorner, H.; Köhler, F. H. *Chem. Ber.* **1973**, *106*, 1122−1128.

(17) Clement, R. A.; Klabunde, U.; Parshall, G. W. *J. Mol. Catal.* **1978**, *4*, 87−94.

(18) Puiu, S. C.; Warren, T. H. *Organometallics* **2003**, *22*, 3974−3976.

(19) Shamir, D.; Zilbermann, I.; Maimon, E.; Cohen, H.; Meyerstein, D. *Inorg. Chem. Commun.* **2007**, *10*, 57−60.

(20) Wright, A. M.; Wu, G.; Hayton, T. W. *J. Am. Chem. Soc.* **2010**, *132*, 14336−14337.

(21) Feltham, R. D. *Inorg. Chem.* **1964**, *3*, 116−119.

(22) Meiners, J. H.; Rix, C. J.; Clardy, J. C.; Verkade, J. G. *Inorg. Chem.* **1975**, *14*, 705−710.

(23) Di Vaira, M.; Ghilardi, C. A.; Sacconi, L. *Inorg. Chem.* **1976**, *15*, 1555−1561.

(24) Kriege-Simondsen, J.; Elbaze, G.; Dartiguenave, M.; Feltham, R. D.; Dartiguenave, Y. *Inorg. Chem.* **1982**, *21*, 230−236.

(25) Onyiriuka, E. C.; Storr, A. *Can. J. Chem.* **1987**, *65*, 1367−1374.

(26) Mar, A.; Rettig, S. J.; Storr, A.; Trotter, J. *Can. J. Chem.* **1988**, *66*, 101−108.

(27) Iluc, V. M.; Miller, A. J. M.; Hillhouse, G. L. *Chem. Commun.* **2005**, 5091−5093.

(28) Landry, V. K.; Pang, K.; Quan, S. M.; Parkin, G. *Dalton Trans.* **2007**, 820−824.

(29) Maffett, L. S.; Gunter, K. L.; Kreisel, K. A.; Yap, G. P. A.; Rabinovich, D. *Polyhedron* **2007**, *26*, 4758−4764.

(30) Fullmer, B. C.; Pink, M.; Fan, H.; Yang, X.; Baik, M.-H.; Caulton, K. G. *Inorg. Chem.* **2008**, *47*, 3888−3892.

(31) Varonka, M. S.; Warren, T. H. *Organometallics* **2010**, *29*, 717−720.

(32) Elbaze, G.; Dahan, F.; Dartiguenave, M.; Dartiguenave, Y. *Inorg. Chim. Acta* **1984**, *87*, 91−97.

(33) Rahman, A. F. M. M.; Salem, G.; Stephens, F. S.; Wild, S. B. *Inorg. Chem.* **1990**, *29*, 5225−5230.

(34) Darensbourg, D. J.; Decuir, T. J.; Stafford, N. W.; Robertson, J. B.; Draper, J. D.; Reibenspies, J. H.; Katho, A.; Joo, F. *Inorg. Chem.* **1997**, *36*, 4218−4226.

(35) Haller, K. J.; Enemark, J. H. *Inorg. Chem.* **1978**, *17*, 3552−3558.

(36) Chong, K. S.; Rettig, S. J.; Storr, A.; Trotter, J. *Can. J. Chem.* **1979**, *57*, 3099−3106.

(37) Chong, K. S.; Rettig, S. J.; Storr, A.; Trotter, J. *Can. J. Chem.* **1979**, *57*, 3090−3098.

(38) MacBeth, C. E.; Thomas, J. C.; Betley, T. A.; Peters, J. C. *Inorg. Chem.* **2004**, *43*, 4645−4662.

(39) Landry, V. K.; Parkin, G. *Polyhedron* **2007**, *26*, 4751−4757.

(40) Tennyson, A. G.; Dhar, S.; Lippard, S. J. *J. Am. Chem. Soc.* **2008**, *130*, 15087−15098.

(41) Gutmann, V. *Coord. Chem. Rev.* **1976**, *18*, 225−255.

(42) Del Zotto, A.; Mezzetti, A.; Novelli, V.; Rigo, P.; Lanfranchi, M.; Tiripicchio, A. *J. Chem. Soc., Dalton Trans.* **1990**, 1035−1042.

(43) Berglund, D.; Meek, D. W. *Inorg. Chem.* **1972**, *11*, 1493−1496.

(44) Bhaduri, S.; Johnson, B. F. G.; Matheson, T. W. *J. Chem. Soc., Dalton Trans.* **1977**, 561−564.

(45) Enemark, J. H.; Feltham, R. D. *Coord. Chem. Rev.* **1974**, *13*, 339−406.

(46) Boyer, M. J. Y.; Rocchiccioli-Deltcheff, C.; Thouvenot, R. *J. Coord. Chem.* **1978**, *7*, 219−226.

(47) Lanfranchi, M.; Pellinghelli, M. A.; Predieri, G.; Bigi, F.; Maggi, R.; Sartori, G. *J. Chem. Soc., Dalton Trans.* **1993**, 1463−1464.

(48) Duffin, B.; Wallwork, S. C. *Acta Crystallogr.* **1966**, *20*, 210−213.

(49) Willett, R. D. *Acta Crystallogr., Sect. E* **2001**, *57*, M53−M54.

(50) Driessen, W. L.; Groeneve, W. *Recl. Trav. Chim. Pays-Bas* **1969**, *88*, 491−498.

(51) Driessen, W. L.; Groeneve, W. *Recl. Trav. Chim. Pays-Bas* **1969**, *88*, 620−624.

(52) Figgis, B. N. *Introduction to Ligand Fields*; John Wiley and Sons: New York, 1966.

(53) Haymore, B.; Feltham, R. D. *Inorg. Synth.* **1973**, *14*, 81−87.

(54) Hieber, W.; Nast, R. *Z. Anorg. Allg. Chem.* **1940**, *244*, 23−47.

(55) Hathaway, B. J.; Holah, D. G.; Underhill, A. E. *J. Chem. Soc.* **1962**, 2444−2448.

(56) Schramm, R. F.; Wayland, B. B. *Chem. Commun.* **1968**, 898−899.

(57) Enemark, J. H. *Inorg. Chem.* **1971**, *10*, 1952−1957.

(58) Bottomley, F.; Brooks, W. V. F.; Clarkson, S. G.; Tong, S.-B. *J. Chem. Soc., Chem. Commun.* **1973**, 919−920.

(59) Bottomley, F. *Acc. Chem. Res.* **1978**, *11*, 158−163.

(60) Velian, A.; Lin, S.; Miller, A. J. M.; Day, M. W.; Agapie, T. *J. Am. Chem. Soc.* **2010**, *132*, 6296−6297.

(61) Meltzer, A.; Präsang, C.; Milsmann, C.; Driess, M. *Angew. Chem., Int. Ed.* **2009**, *48*, 3170−3173.

(62) Nickel, T.; Goddard, R.; Krüger, C.; Pörschke, K.-R. *Angew. Chem., Int. Ed.* **1994**, *33*, 879−882.

(63) Lee, C. H.; Laitar, D. S.; Mueller, P.; Sadighi, J. P. *J. Am. Chem. Soc.* **2007**, *129*, 13802−13803.

(64) Watanabe, C.; Inagawa, Y.; Iwamoto, T.; Kira, M. *Dalton Trans.* **2010**, *39*, 9414−9420.

(65) Brunner, H. *J. Organomet. Chem.* **1968**, *12*, 517−522.

(66) Chen, L. X.; Bowman, M. K.; Wang, Z.; Montano, P. A.; Norris, J. R. *J. Phys. Chem.* **1994**, *98*, 9457−9464.

(67) Fomitchev, D. V.; Furlani, T. R.; Coppens, P. *Inorg. Chem.* **1998**, *37*, 1519−1526.

(68) *SMART Software Users Guide*, version 5.1; Bruker Analytical X-ray Systems, Inc.: Madison, WI, 1999.

(69) *SAINT Software Users Guide*, version 5.1; Bruker Analytical X-ray Systems, Inc.: Madison, WI, 1999.

(70) Sheldrick, G. M. *SHELXTL*, version 6.12; Bruker Analytical X-ray Systems, Inc.: Madison, WI, 2001.